ELSEVIER

Journal of Fluids and Structures 25 (2009) 263–283

JOURNAL OF FLUIDS AND STRUCTURES

www.elsevier.com/locate/jfs

A numerical study on the flow patterns of two oscillating cylinders

Dae Sung Lee[a], Man Yeong Ha[b,*], Hyun Sik Yoon[c], S. Balachandar[d]

[a]*Supercomputing Center, Korea Institute of Science and Technology Information (KISTI), 335 Gwahangno, Yuseong-gu, Daejeon 305-806, Republic of Korea*

[b]*Department of Mechanical Engineering, Pusan National University, Jang Jeon 2-Dong, Geum Jeong Gu, Busan 609-735, Republic of Korea*

[c]*Advanced Ship Engineering Research Center, Pusan National University, Jang Jeon 2-Dong, Geum Jeong Gu, Busan 609-735, Republic of Korea*

[d]*Mechanical & Aerospace Engineering, University of Florida, 231 MAE-A, P.O. Box 116250, Gainesville, FL 32611-6250, USA*

Received 28 May 2007; accepted 16 June 2008
Available online 13 December 2008

Abstract

Flow around two oscillating cylinders in a side-by-side arrangement at Reynolds number (Re) = 185 is simulated using the immersed boundary method. The purpose of this study is to investigate the combined effects of the gap between the two cylinders and their oscillation in the flow. The cylinders oscillate transversely to a uniform cross-flow with a prescribed sinusoidal function in the opposite direction, with the oscillation amplitude equal to 20% of the cylinder diameter. The gap between the two cylinders and the oscillating frequency are chosen as major variables for the parametric study to investigate their influence on the flow pattern. The ratio of mean gap distance between the two oscillating cylinders to the cylinder diameter is chosen to be 0.6, 1.0, 1.4, and 1.8, and the ratio of oscillating frequencies to the natural vortex shedding frequency of a fixed cylinder is 0.8, 1.0, and 1.2. Wake patterns and the drag and lift coefficients are described and compared with those from a single oscillating cylinder and two stationary cylinders. The wake patterns of two oscillating cylinders can be explained by flow mechanisms of two stationary cylinders, a single oscillating cylinder, and their combinations, and are in agreement with classifications of flow over two stationary cylinders presented in previous studies. In the case of two oscillating cylinders, the modulation phenomenon appears from a lower excitation frequency than in a single oscillating cylinder. Generally, oscillating cylinders have higher drag and root-mean-square (r.m.s.) values of drag coefficients than stationary cylinders.

Keywords: Two cylinders; Forced oscillation; Wake pattern; Immersed boundary method

1. Introduction

There is extensive literature on flow over a cylinder, as it is an important problem for academic and engineering purposes. For instance, the tube bundle for heat exchangers is an example of multiple cylinders, and some experience

*Corresponding author. Tel.: +82 51 510 2440; fax: +82 51 512 9835.
E-mail address: myha@pusan.ac.kr (M.Y. Ha).

0889-9746/$ - see front matter © 2008 Elsevier Ltd. All rights reserved.
doi:10.1016/j.jfluidstructs.2008.06.011

flow-induced vibrations. In addition, oscillating cylinders in cross or stationary flow are frequently observed in offshore structures and power cables with fluid–structure interactions. Building on the understanding of flow over a single stationary cylinder, many researchers have recently focused attention on multiple stationary or oscillating cylinders. Flow around two oscillating cylinders is expected to have characteristics of both an oscillating cylinder and multiple cylinders. Thus, the cases of single oscillating cylinder and two stationary cylinders are focused on for the literature survey below.

Flow past a single oscillating cylinder has been investigated in several previous studies, including experimental studies by Toebes (1969), Gu et al. (1994) and Williamson and Roshko (1988), and numerical investigations by Meneghini and Bearman (1995), Blackburn and Henderson (1999), Anagnostopoulos (2000), Guilmineau and Queutey (2002), Ponta and Aref (2006) and Leontini et al. (2006) (see Khalak and Williamson (1999) for further references).

Williamson and Roshko (1988) analyzed the wake patterns behind an oscillating cylinder at low Reynolds numbers. The two main parameters that determine the wake patterns are the amplitude of oscillation and the frequency ratio (trajectory wavelength of the cylinder over its diameter). They described the formation of vortices and shedding in detail along the moving cylinder. In the fundamental lock-in regime, the oscillating cylinder sheds four vortices during each cycle. They classified the wake patterns with a 'P' for a vortex pair and a 'S' for a single vortex. Below a critical trajectory wavelength, the cylinder creates a 2S mode of the Karman street-type vortex. If the wavelength is increased over a critical value, the cylinder sheds two like-signed vortex pairs (2P mode).

Gu et al. (1994) experimentally investigated the flow over an oscillating cylinder for Reynolds numbers of 185 and 5000. The frequency ratio, which is defined as the ratio of the oscillating frequency to the natural vortex shedding frequency of the fixed cylinder, ranged from 0.8 to 1.2. As the frequency ratio increases, the vortex formation length decreases, and if the frequency ratio increases over 1.12, a switch in the vortex formation position occurs which persists up to a frequency ratio of 1.2.

Guilmineau and Queutey (2002) numerically simulated the flow over an oscillating cylinder at $\mathrm{Re} = 185$ to reproduce the experimental results of Gu et al. (1994). They also observed the vortex switching phenomenon and explained it with detailed numerical data such as the distribution of vorticity and pressure along the cylinder and the r.m.s. of streamwise velocity at the centerline.

The flow over two stationary cylinders in a side-by-side arrangement is another problem relevant to the present study. Kim and Durbin (1988) experimentally studied the wake at $\mathrm{Re} = 2 \times 10^3$ for a gap spacing (g) of 0.75, where g is the distance between two cylinders normalized by the cylinder diameter. The wakes flip-flop randomly between two asymmetric states. The time-scale for the flip-flopping is several orders of magnitude longer than that of vortex shedding.

Sumner et al. (1999) investigated flow in the range of $\mathrm{Re} = 500$–3000 and $g = 0$–5 and identified three basic wake patterns that were insensitive to the Reynolds number (Re) : single-bluff-body vortex shedding at small gap spacings ($0 \leqslant g < 0.2$), biased flow with synchronized vortex shedding at intermediate spacings ($0.2 \leqslant g \leqslant 1.2$), and symmetric flow with synchronized vortex shedding at larger spacings ($1.2 < g \leqslant 3.5$).

Recently, Kang (2003) investigated flow over two stationary cylinders in a side-by-side arrangement at $40 \leqslant \mathrm{Re} \leqslant 160$ and with $g < 5$. He classified six wake patterns, including 'anti-phase synchronized' ($g \geqslant 2$), 'in-phase synchronized' ($g \geqslant 1.5$), 'flip-flopping' ($0.4 \leqslant g \leqslant 1.5$), 'single bluff-body' ($g \leqslant 0.4$), 'deflected' ($50 \leqslant \mathrm{Re} \leqslant 110$ and $0.2 \leqslant g \leqslant 1$), and 'steady' ($\mathrm{Re} \leqslant 40$ and $g \geqslant 0.5$) wake patterns. These wake patterns in the laminar regime, which are affected by gap spacing more than by Reynolds number, are illustrated in detail along with drag and lift coefficients.

Oscillating cylinders show lock-in phenomena and various wake patterns as a function of oscillation frequency and amplitude. In the case of multiple stationary cylinders, the different shed vortices interfere with the interaction, depending on the gap between the two cylinders. Thus, the flow characteristics of two oscillating cylinders may differ from those of two stationary cylinders and one oscillating cylinder. Therefore, in this study, the gap spacing between the two cylinders and their oscillation frequency are chosen as the basic variables for the parametric study.

There are few previous studies of flow over two oscillating cylinders. Mahir and Rockwell (1996) experimentally studied the flow over two oscillating cylinders in a side-by-side arrangement in a cross-flow. The two cylinders oscillated independently with phase-change between the position of the two cylinders at $\mathrm{Re} = 160$. They varied the frequency ratio, the phase angle, and the amplitude. At low frequency ratios, the natural vortex shedding frequency of the two fixed cylinders appeared as a distinctive peak. As the frequency ratio increases, the oscillation frequency dominates, while the natural shedding frequency fades. They also changed the phase angle at the same frequency and observed the transformation from modulated to lock-in response.

Jester and Kallinderis (2004) numerically simulated two oscillating cylinders in a side-by-side arrangement at $\mathrm{Re} = 160$ and compared the wake patterns with those from Mahir and Rockwell (1996), however, they gave no detailed results on the flow field or other quantitative information.

The objective of this study is to investigate the characteristics of flow over two oscillating cylinders in comparison with those of a single oscillating cylinder and of two stationary cylinders. Here, the two cylinders in a side-by-side arrangement oscillate alternately towards and away from each other, out-of-phase, in a cross-flow at Re = 185. The dependency of the wake, drag, and lift coefficients on the frequency ratio and the gap spacing is the primary focus of this study.

2. Numerical method

2.1. Governing equations

Fig. 1 shows the computational domains and boundary conditions considered in this study. The governing equations describing instantaneous incompressible viscous flow in the dimensionless form are given by the continuity and the momentum equations as follows:

$$\frac{\partial u_i}{\partial x_i} - q = 0, \tag{1}$$

$$\frac{\partial u_i}{\partial t} + \frac{\partial u_i u_j}{\partial x_j} = -\frac{\partial p}{\partial x_i} + \frac{1}{\mathrm{Re}}\frac{\partial^2 u_i}{\partial x_j \partial x_j} + f_i, \tag{2}$$

where q and f_i are the mass sink/source and the momentum forcing, respectively, for the immersed boundary method (Kim et al., 2001).

Normalization of Eqs. (1) and (2) using the cylinder diameter D and the free-stream velocity U_∞ results in the dimensionless parameter of Reynolds number $\mathrm{Re} = U_\infty D/v$. A finite volume method is used in the present study, where the second-order two-step fractional step method is employed for time advancement. This scheme was used previously by Kim and Moin (1985) and Zang et al. (1994). The nonlinear terms are treated explicitly using the second-order Adams–Bashforth scheme, and diffusion terms are treated implicitly using the Crank–Nicolson scheme.

2.2. Computational details

The computational domain is chosen to be $-40 < x < 50$ and $-40 < y < 40$. The Dirichlet condition for velocity is applied at the inlet and at the top and bottom walls with $u = 1$, $v = 0$, where u and v are the x and y components of velocity, respectively. A convective flow condition, $\partial u_i/\partial t + c\partial u_i/\partial x = 0$ (c is the average streamwise velocity at the outlet), is adopted for the outlet. A grid of 900×682 grid points with a fine grid ($\Delta x = 0.01$, $\Delta y = 0.01$) near the oscillating cylinder is used. The condition of CFL < 0.3 is used to determine the nondimensional time step used in the calculations, and as a result a time step of 0.001 is used for all the calculations.

Previous numerical studies regarded the flow around an oscillating cylinder near Re = 185 as two-dimensional (2-D) even though it may be three-dimensional (3-D) flow for a stationary cylinder (Blackburn and Henderson, 1999; Guilmineau and Queutey, 2002). According to Blackburn and Henderson (1999), as the spanwise correlations of forces

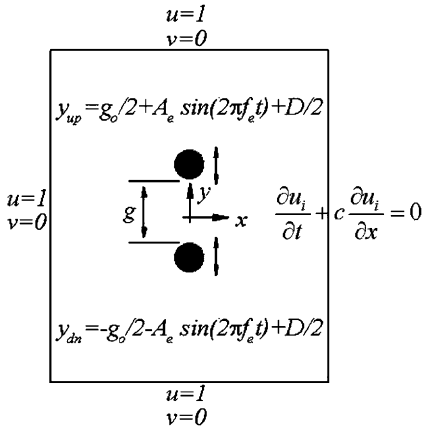

Fig. 1. Computational domain and boundary conditions.

and wake velocities increase with increasing cylinder motion amplitude, it is reasonable to suggest that the harmonic motion of a long circular cylinder will suppress the 3-D effects and produce flows that are more 2-D than their fixed-cylinder counterparts, at least in the near-wake region. For two cylinders, there may be no critical errors in the 2-D flow assumption at about $g>0.4$ (Kang, 2003). In this study, two oscillating cylinders are implemented with the immersed boundary method (Kim et al., 2001). The advantage of the immersed boundary method is that even as the cylinders move, the grid does not need to be re-generated.

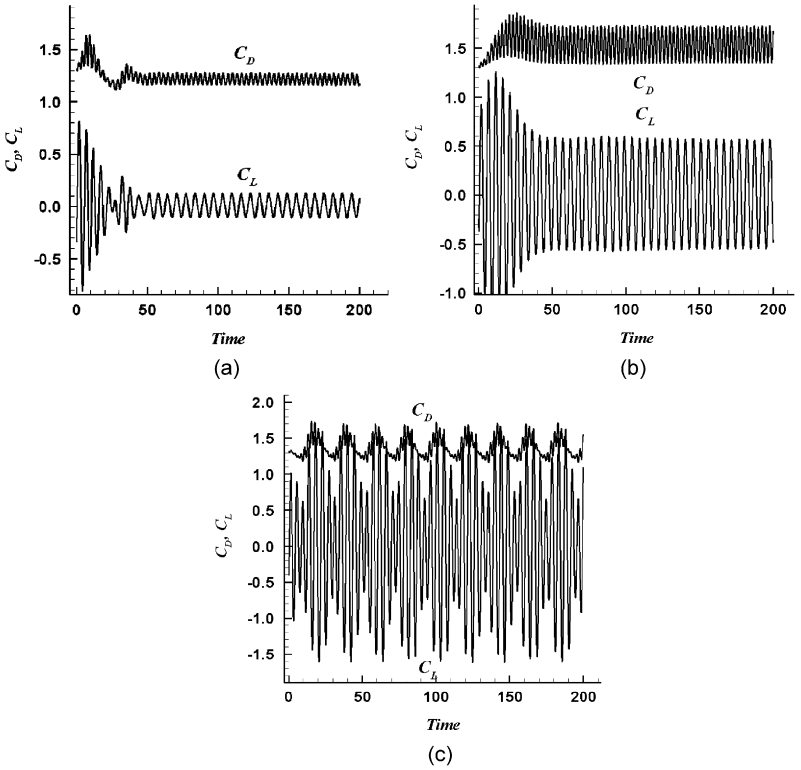

Fig. 2. Drag and lift coefficients as a function of time for one oscillating.

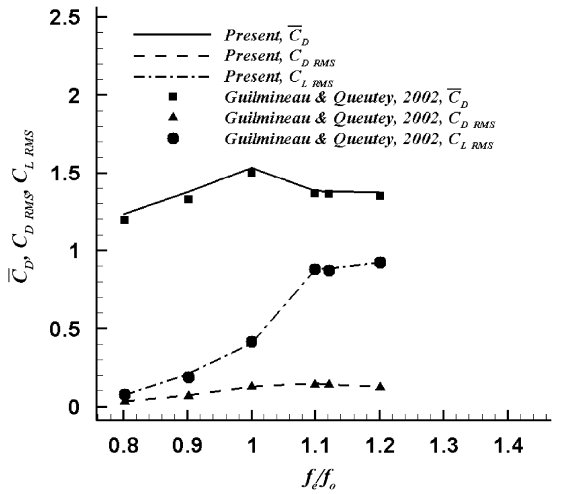

Fig. 3. Time-averaged drag and r.m.s. of drag and lift coefficients for one oscillating cylinder at Re = 185. Results from this study are compared with those from Guilmineau and Queutey (2002).

2.3. Important parameters

As shown in Fig. 1, the out-of-phase periodic oscillations of the two cylinders are governed by the following equations:

$$y_{up} = \frac{g_o}{2} + \frac{D}{2} + A_e \sin(2\pi f_e t), \quad y_{dn} = \frac{-g_o}{2} + \frac{D}{2} - A_e \sin(2\pi f_e t) \tag{3,4}$$

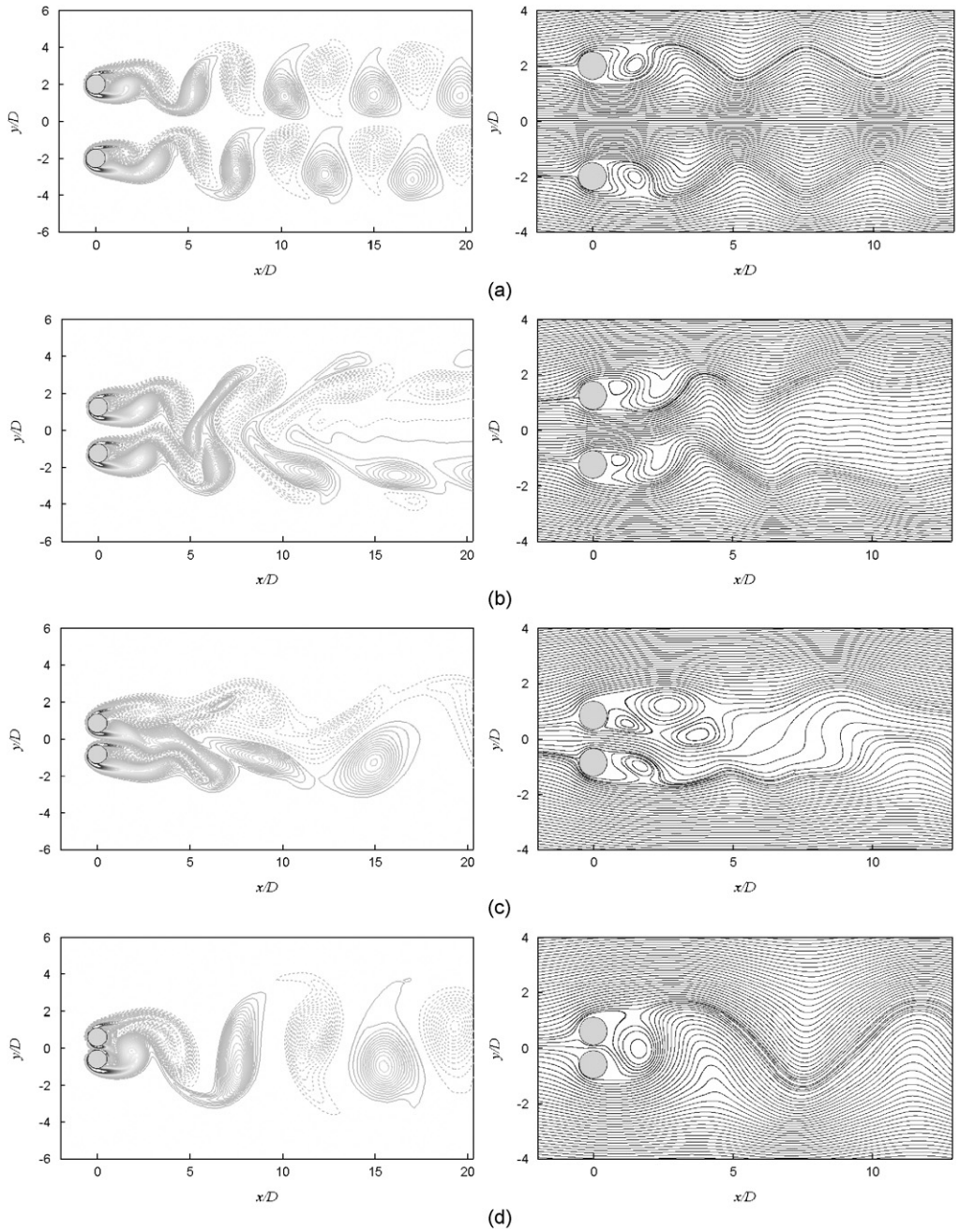

Fig. 4. Instantaneous vorticity contours (left column) and streamlines (right column) for various gap spacings at Re = 100: (a) $g = 3.0$, (b) $g = 1.5$, (c) $g = 0.7$, and (d) $g = 0.2$.

where A_e is the oscillation amplitude, which in the present simulations is chosen to be 0.2, y_{up} and y_{dn} are the centers of the upper and lower cylinders, respectively, f_o is the natural frequency of one cylinder when held fixed at Re = 185, f_e is the excitation frequency, and g_o is the mean value of the gap between the two oscillating cylinders. Thus, the gap (g)

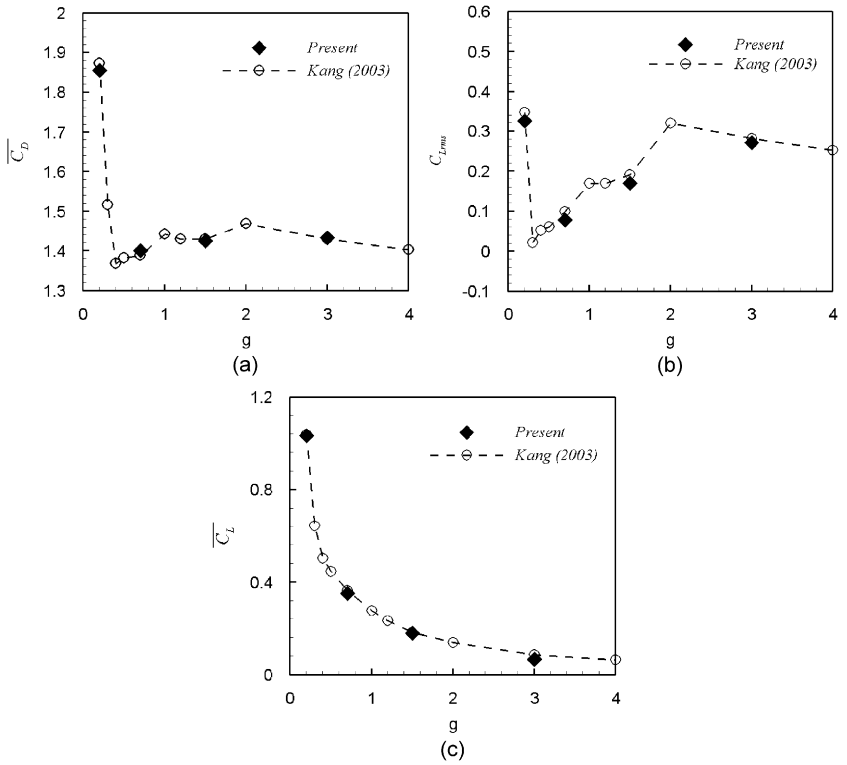

Fig. 5. Variation of the time-averaged and r.m.s. values of lift and drag coefficients at Re = 100.

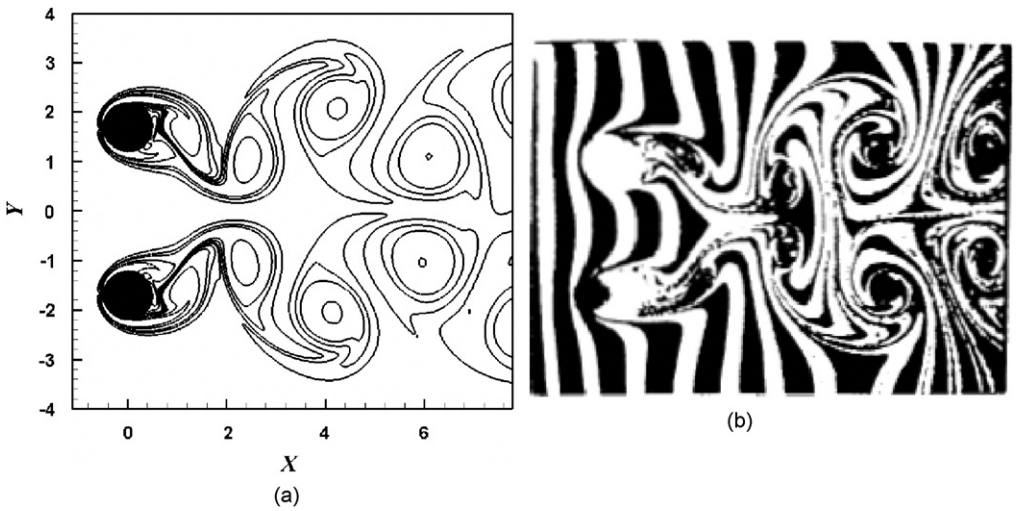

Fig. 6. Instantaneous vorticity contours of two oscillating cylinders at Re = 160, $g_o = 2$, $A_e = 0.2$, and $f_e/f_o{}^{**} = 1.0$. (a) present result, (b) results from Mahir and Rockwell (1996).

between the oscillating cylinders is $(g_o-0.4)\leqslant g\leqslant(g_o+0.4)$. The natural frequency f_o is 0.192, which was determined from the simulation of one fixed cylinder.

3. Validations

Three different problems are considered to validate the numerical simulation method. First, flow around a single oscillating cylinder is simulated at $\mathrm{Re}=185$, $A_e=0.2$, and $f_e/f_o=0.8$–1.2. Time histories of the drag and lift coefficients for $f_e/f_o=0.8$, 1.0, and 1.2 are presented in Fig. 2. For $f_e/f_o=0.8$ and $f_e/f_o=1.0$, the drag and lift coefficients show regular sinusoidal variations, and the oscillation amplitude for $f_e/f_o=1.0$ is larger than that for $f_e/f_o=0.8$. For $f_e/f_o=1.2$, the drag and lift coefficients have a low frequency modulation. These characteristics are

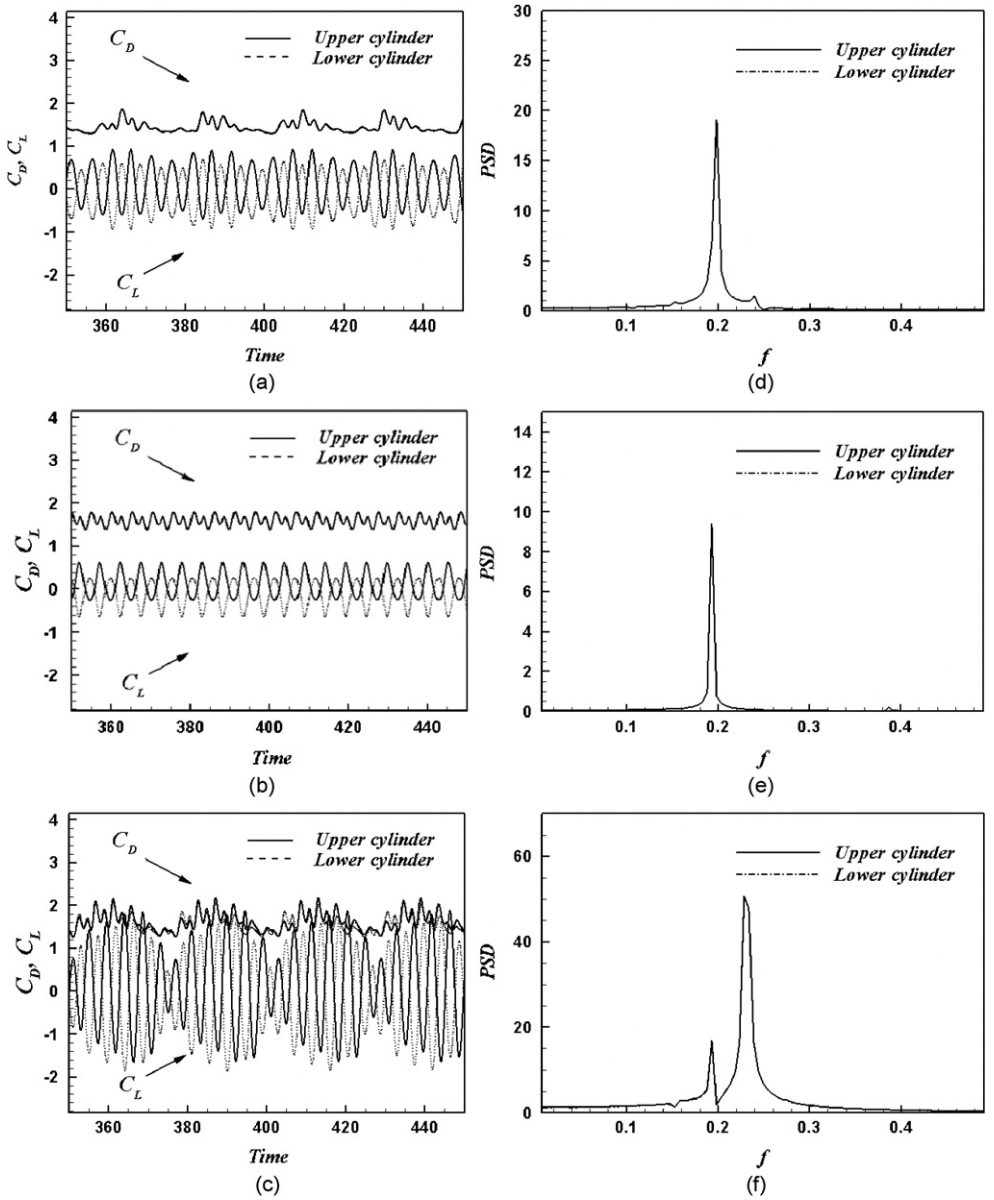

Fig. 7. Drag and lift coefficients (left column) and power spectrum of lift coefficients (right column) for $g_o=1.8$. In (a) and (d), $f_e/f_o=0.8$; in (b) and (e), $f_e/f_o=1.0$; in (c) and (f), $f_e/f_o=1.2$.

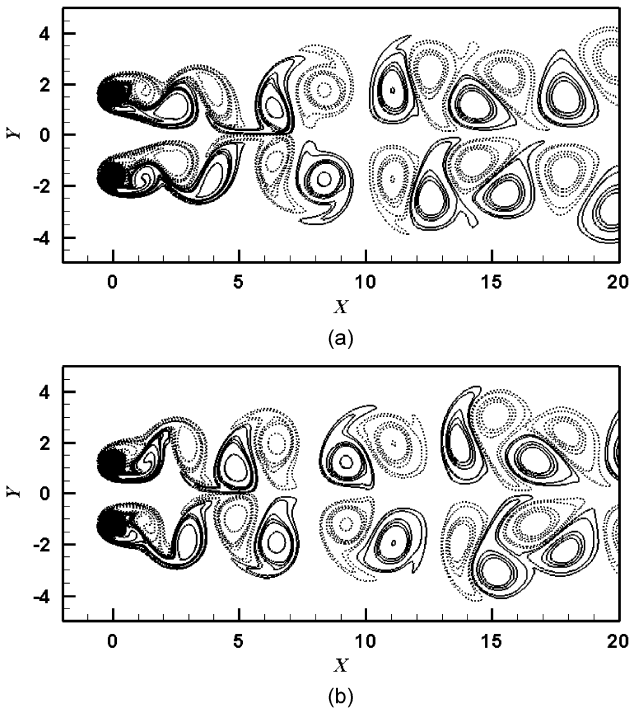

Fig. 8. Time series of instantaneous vorticity fields for $g_o = 1.8$ and $f_e/f_o = 0.8$ for (a) the furthest positions and (b) the closest positions.

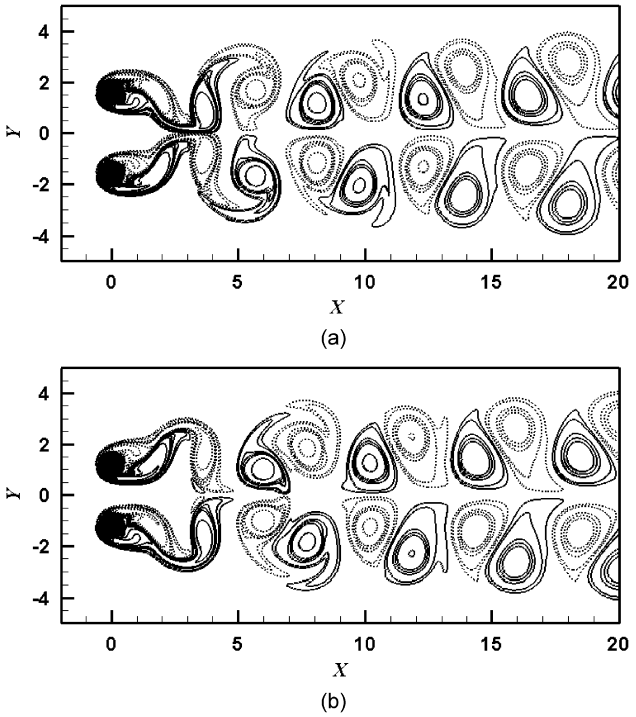

Fig. 9. Time series of instantaneous vorticity fields for $g_o = 1.8$ and $f_e/f_o = 1.0$ for (a) the furthest positions and (b) the closest positions.

consistent with the findings of Guilmineau and Queutey (2002). In addition, the mean drag and r.m.s. of the drag and lift coefficients agree well with those of Guilmineau and Queutey (2002), as shown in Fig. 3.

In the case of two stationary cylinders, we follow the study of Kang (2003). At Re = 100, two stationary cylinders were simulated for gaps of 3.0, 1.5, 0.7, and 0.2. In Fig. 4, instantaneous vorticity fields and streamlines show the anti-phase-synchronized pattern for $g = 3.0$, in-phase synchronized pattern for $g = 1.5$, flip-flop pattern for $g = 0.7$, and single bluff-body pattern for $g = 0.2$. These results show good agreement with Kang (2003). Time-averaged drag and lift coefficients and r.m.s. of lift coefficients as the mean value between two cylinders are plotted in Fig. 5, and are in good agreement with Kang (2003).

For two oscillating cylinders, we confirm the present numerical method of simulating the relative motion of multi-bodies by following Mahir and Rockwell's (1996) experimental conditions of Re = 160, $A_e = 0.2$, $g_o = 2$, and $f_e/f_o^{**} = 1.0$, where f_o^{**} is the natural vortex shedding frequency of the two fixed cylinders. The parallel anti-phase streets of vortices obtained from the present computation are in good agreement with the results of Mahir and Rockwell (1996), as shown in Fig. 6.

4. Results

4.1. Wake patterns

4.1.1. $g_o = 1.8$

For $g_o = 1.8$, which corresponds to the largest dimensionless gap between the two cylinders considered in this study, the two cylinders oscillate out of phase. According to Kang (2003), wake patterns for two stationary cylinders with a gap $g_o = 1.8$ at Re = 185 show 'anti- or in-phase synchronized' patterns.

Fig. 7 shows the time evolution of the drag and lift coefficients for the upper and lower cylinders for $g_o = 1.8$ and the power spectrum of the lift coefficients. Throughout this paper, a solid line is used for the upper cylinder and a dashed line for the lower cylinder. For $f_e/f_o = 0.8$ (Fig. 7(a)), drag coefficients of the upper and lower cylinders are the same in magnitude and pattern and show the signs of modulation. The lift coefficients for the two cylinders are 'anti-phase

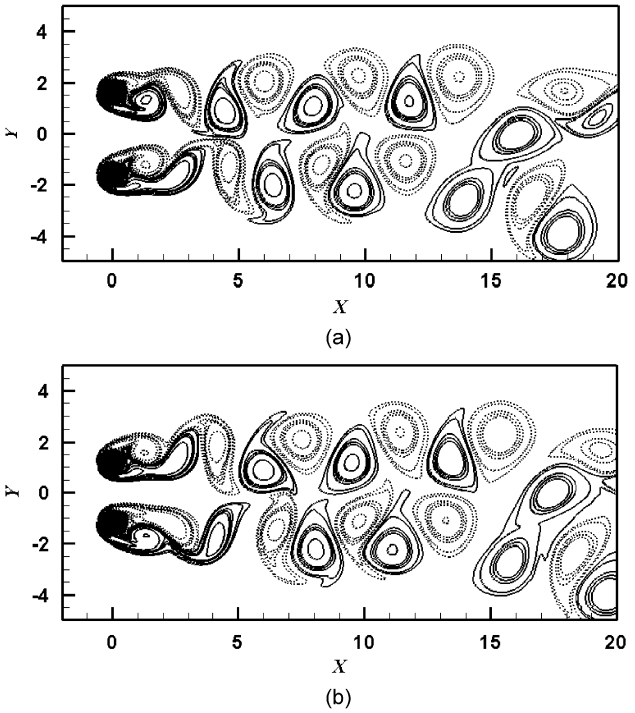

Fig. 10. Time series of instantaneous vorticity fields for $g_o = 1.8$ and $f_e/f_o = 1.2$ for (a) the furthest positions and (b) the closest positions.

synchronized'. Modulation does not appear for the single oscillating cylinder at $f_e/f_o = 0.8$ or for the two stationary cylinders for $g_o = 1.8$. However, when those conditions are combined, modulation appears because of interference of symmetric vortices from the two cylinders (see Figs. 2 and 4 for the single oscillating and two stationary cylinders, respectively). Lift coefficients show symmetry, as two stationary cylinders do for $g_o = 1.8$.

For $f_e/f_o = 1.0$ (Fig. 7(b)), drag and lift coefficients show periodicity. The drag coefficients of the upper and lower cylinders are the same and lift coefficients show corresponding symmetry. They are also 'anti-phase synchronized'. As the oscillation frequency is increased to 1.2 (Fig. 7(c)), the drag coefficients of the upper and lower cylinders show a minor discrepancy between them, and the lift coefficients also show small deviations in symmetry. They alternately show 'anti-phase synchronized' and 'deflected' patterns. They also show modulation phenomena as appeared in $f_e/f_o = 0.8$. The Fourier transformations of the lift coefficients, shown in Fig. 7(d–f), have primary peaks at f_o for $f_e/f_o = 0.8$ and at $f_o = f_e$ for $f_e/f_o = 1.0$. For $f_e/f_o = 1.2$, it shows one primary peak at $f \approx f_e$ and a secondary peak at $f \approx f_o$. In this study, lock-in is judged if the primary frequency of the lift coefficient is the same as that of the body motion

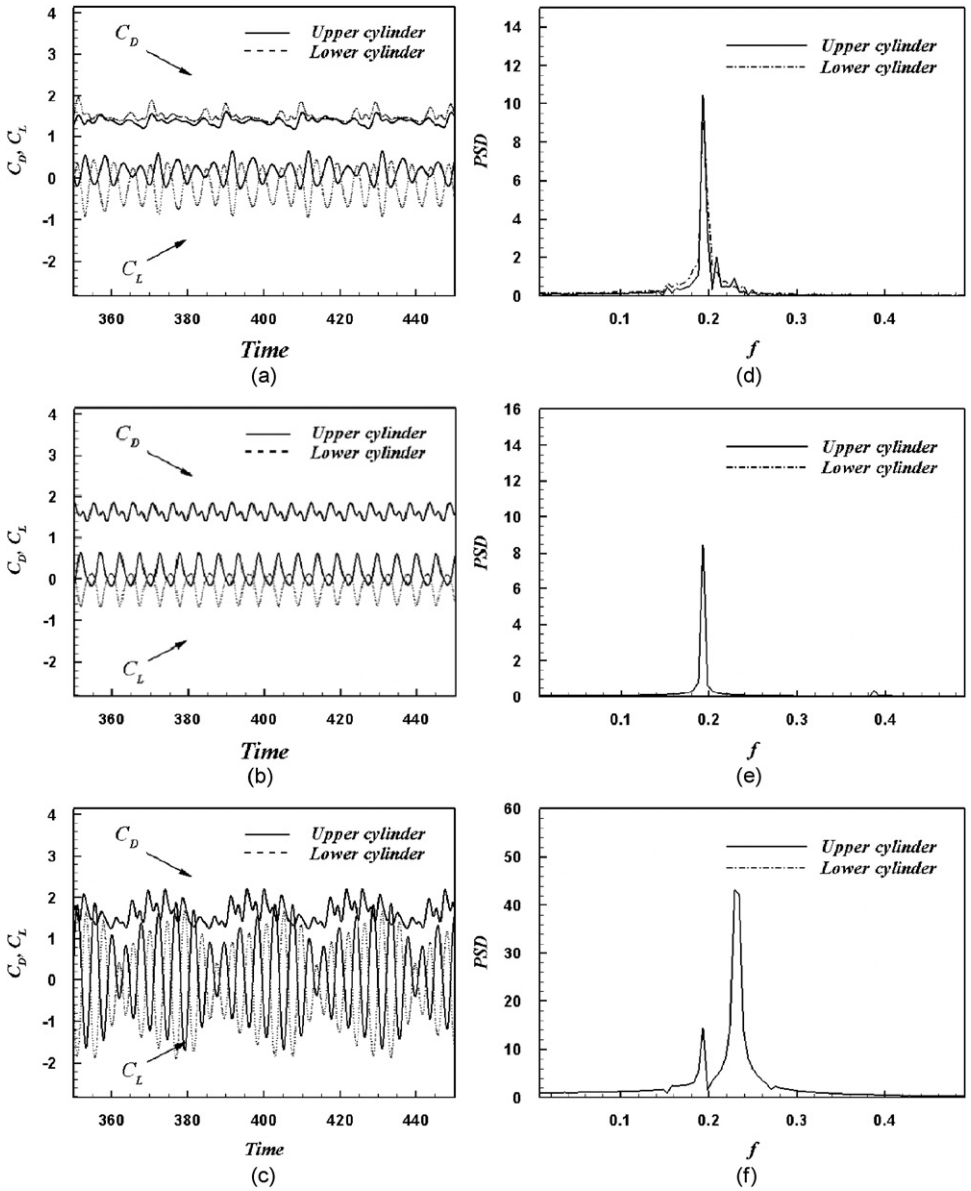

Fig. 11. Drag and lift coefficients (left column) and power spectra of lift coefficients (right column) for $g_o = 1.4$. In (a) and (d), $f_e/f_o = 0.8$; in (b) and (e), $f_e/f_o = 1.0$; in (c) and (f), $f_e/f_o = 1.2$.

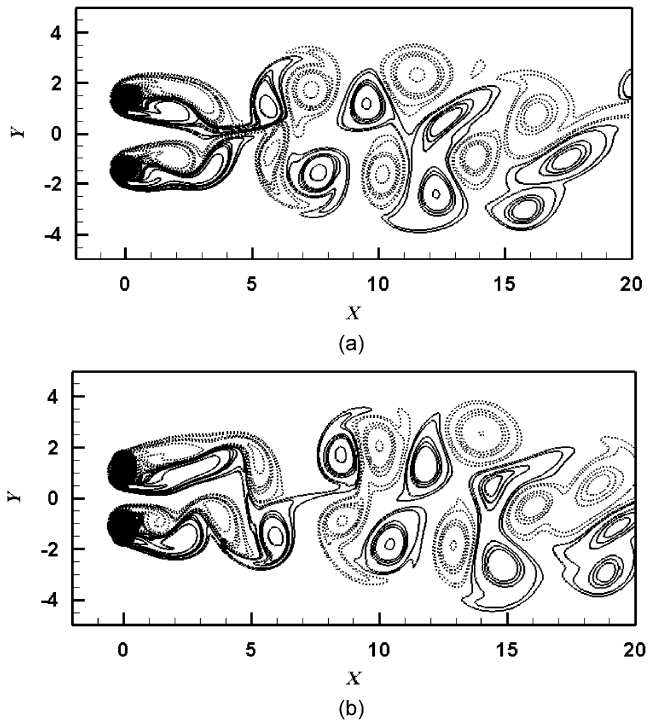

Fig. 12. Time series of instantaneous vorticity fields for $g_o = 1.4$ and $f_e/f_o = 0.8$ for (a) the furthest positions and (b) the closest positions.

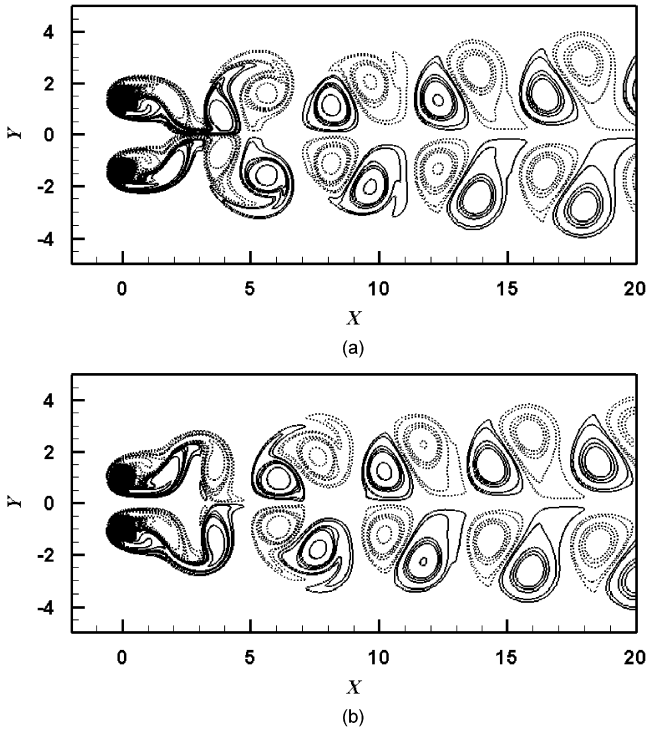

Fig. 13. Time series of instantaneous vorticity fields for $g_o = 1.4$ and $f_e/f_o = 1.0$ for (a) the furthest positions and (b) the closest positions.

frequency. Thus, $f_e/f_o = 1.2$ is in the 'lock-in' regime and others are not. As the power spectra of the upper and lower cylinders are the same, only a solid line can be seen in Fig. 7(d–f).

Fig. 8 shows the instantaneous vorticity fields of the two oscillating cylinders when they are furthest and closest to each other. Anti-phase synchronized vortices form two parallel anti-phase streets that are symmetric about the wake centerline. The structure of wake pattern remains symmetric downstream without merging or distortion of the vortices. The vortex shedding of upper and lower cylinders interferes and the vortex shedding pattern is different from that of one oscillating cylinder.

Fig. 9 shows the instantaneous vorticity fields for $f_e/f_o = 1.0$. Unlike $f_e/f_o = 0.8$, $f_e/f_o = 1.0$ has the same pattern at both the furthest and the closest positions. The lateral (streamwise) vortex formation length and lateral gap between the shed vortices remain constant. The vortices in the wake keep their symmetric form until far downstream, without merging or distortion. Fig. 10 shows the instantaneous vorticity for $f_e/f_o = 1.2$. The vortices are asymmetric and some merge and are distorted while flowing downstream. Thus, for $g_o = 1.8$, 'in-phase synchronized' and 'deflected' pattern are found for $0.8 \leqslant f_e/f_o \leqslant 1.2$.

4.1.2. $g_o = 1.4z$

This range includes the flip-flop and 'anti- or in-phase synchronized' wake patterns for two stationary cylinders (Kang, 2003). Time histories of drag and lift coefficients of two oscillating cylinders are depicted in Fig. 11. At $f_e/f_o = 0.8$ (Fig. 11(a)), the drag and lift coefficients are modulated, as in the case of $g_o = 1.8$ and $f_e/f_o = 0.8$ (Fig. 7(a)). However, drag coefficients of the upper and lower cylinders are not the same, and the lift coefficients of the upper and lower cylinders are not symmetric. They show 'anti-phase synchronized' and 'deflected' patterns. When $f_e/f_o = 1.0$, the drag and lift coefficients (Fig. 11(b)) have nearly the same characteristics as the case of $g_o = 1.8$ (Fig. 9). They are also 'anti-phase synchronized'. As the oscillating frequency is increased to 1.2 (Fig. 11(c)), symmetric lift coefficients are observed, while for the wider gap of $g_o = 1.8$ and $f_e/f_o = 1.2$ we previously observed asymmetry. The drag coefficients of the two cylinders are the same, while for $g_o = 1.8$ at the same frequency ratio, the drag for the two cylinders shows a discrepancy. The Fourier transforms of lift coefficients for $g_o = 1.4$ are shown in Fig. 11(d–f), and show characteristics similar to the case of $g_o = 1.8$. The spectra have primary peaks at f_o for $f_e/f_o = 0.8$ and 1.0 and at f_e for $f_e/f_o = 1.2$.

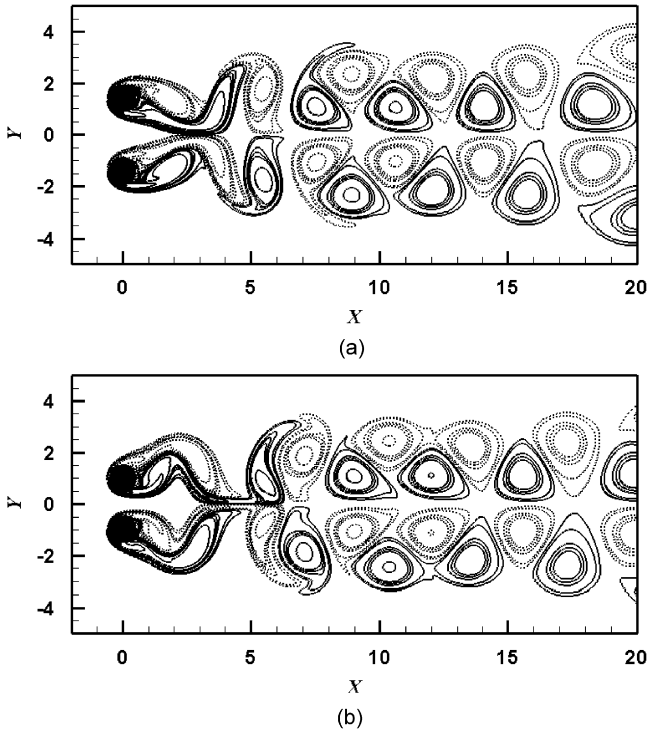

Fig. 14. Time series of instantaneous vorticity fields for $g_o = 1.4$ and $f_e/f_o = 1.2$ for (a) the furthest positions and (b) the closest positions.

Because of mutual interference of vortices, the wake patterns shown in the instantaneous vorticity fields (Fig. 12) appear to be the 'deflected' pattern rather than the 'flip-flop' pattern that appears for two stationary cylinders at $g_o = 1.4$. Kang (2003) inferred that the deflected wake pattern should be another kind of flip-flop pattern with an extremely large flip-flopping time scale, as mentioned in Kim and Durbin (1988). Thus, the wake patterns of the upper and lower cylinders can be switched with extremely large simulation time. When $f_e/f_o = 1.0$, the characteristics of the vortices for $g_o = 1.4$ are the same as for $g_o = 1.8$, as can be seen in Figs. 9 and 13.

Fig. 14 shows the instantaneous vorticity fields for $f_e/f_o = 1.2$. A symmetric wake pattern is observed and merging between vortices occurs only in the flow direction. Generally, vortices shed with short streamwise vortex lengths maintain their shape well, while long vortices easily deform and merge as they flow downstream. At $f_e/f_o = 1.2$, all characteristics for $g_o = 1.4$ are similar to those of $g_o = 1.8$ except the symmetry of flow pattern. In summary, for $g_o = 1.4$, 'in-phase synchronized' and 'deflected' patterns are found for $0.8 \leqslant f_e/f_o \leqslant 1.2$.

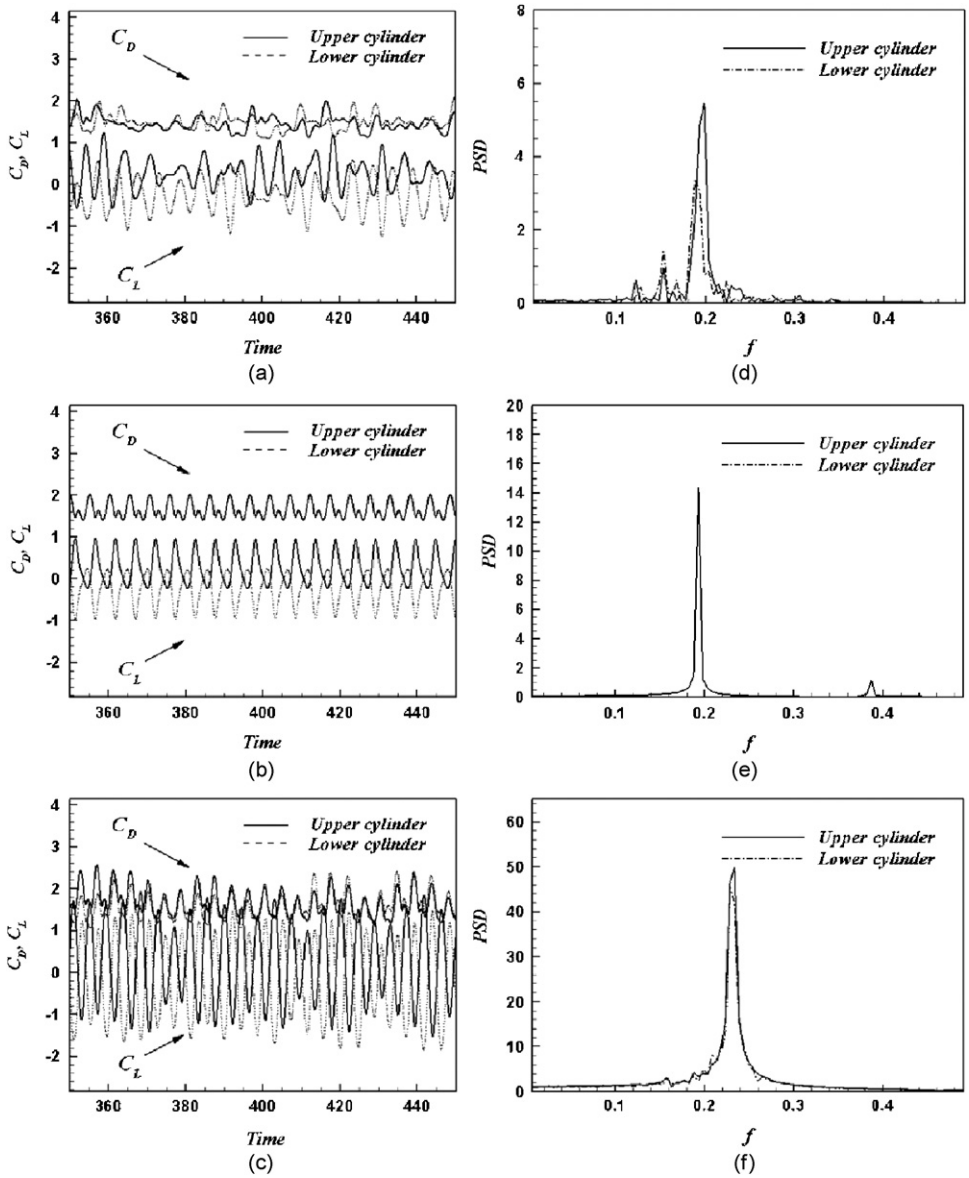

Fig. 15. Drag and lift coefficients (left column) and power spectrum of lift coefficients (right column) for $g_o = 1$. In (a) and (d), $f_e/f_o = 0.8$; in (b) and (e), $f_e/f_o = 1.0$; in (c) and (f), $f_e/f_o = 1.2$.

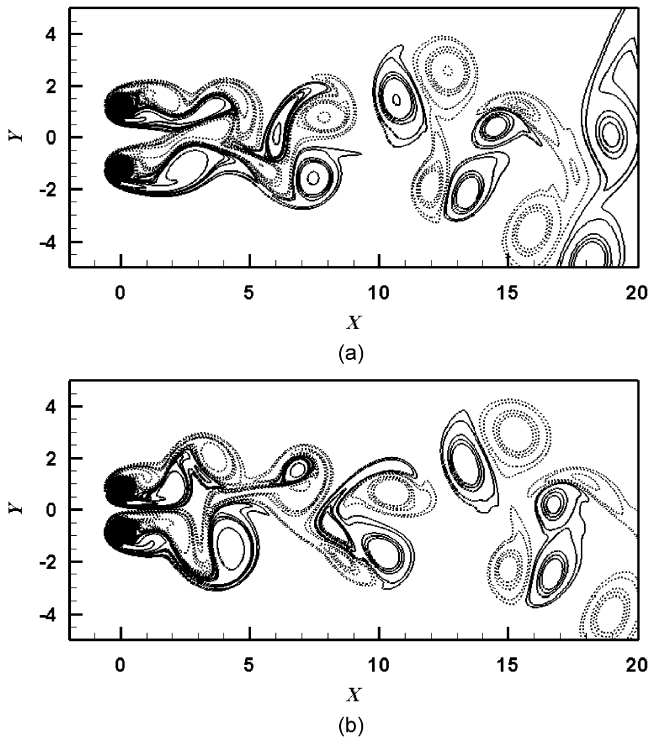

Fig. 16. Time series of instantaneous vorticity fields for $g_o = 1$ and $f_e/f_o = 0.8$ for (a) the furthest positions and (b) the closest positions.

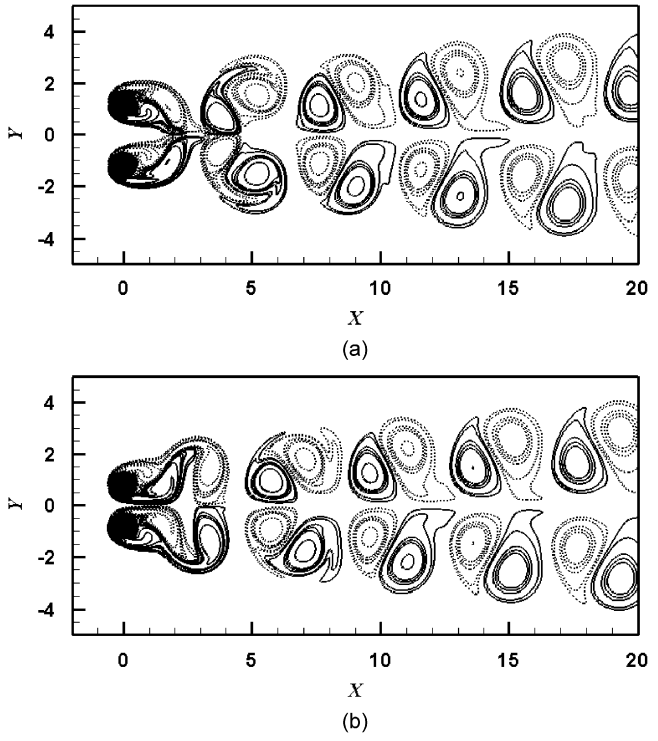

Fig. 17. Time series of instantaneous vorticity fields for $g_o = 1$ and $f_e/f_o = 1.0$ for (a) the furthest positions and (b) the closest positions.

4.1.3. $g_o = 1$

The flow characteristics at $g_o = 1$ include 'flip-flop' and 'anti- or in-phase synchronized' wake patterns for two stationary cylinders (Kang, 2003). Fig. 15(a) shows the drag and lift coefficients when $f_e/f_o = 0.8$. Their patterns for $g_o = 1$ are more irregular than those for $g_o = 1.4$. A flip-flop pattern can be found in the drag coefficients, but anti- or in-phase synchronized patterns cannot be found. The Fourier transform of the lift coefficients are presented in Fig. 15(d) and show a primary peak at $f \approx f_o$. When $f_e/f_o = 1.0$, the patterns of the drag and lift coefficients for $g_o = 1$ (Fig. 15(b)) are similar to the cases of $g_o = 1.8$ and $g_o = 1.4$. They show an anti-phase synchronized pattern. The primary peak shown in Fig. 15(e) is at f_e. A weak modulation can be discerned for $f_e/f_o = 1.2$, as shown in Fig. 15(c), and the primary peak shown in Fig. 15(f) is at f_e. As the gap between the two cylinders is decreased, symmetry in lift coefficients and the simultaneity of drag coefficients between the upper and lower cylinders cannot be found, except for $f_e/f_o = 1.0$.

Fig. 16 shows the instantaneous vorticity fields for $g_o = 1$ and $f_e/f_o = 0.8$. The furthest position has a deflected near wake pattern and the closest position has a symmetric pattern only in the near wake. Vortices shed from the cylinders are distorted and merged in the near wake, forming complex and random wake patterns and with unclear periodicity. When the cylinders are in the closest position, they are so close that vortex shedding interferes with each other. Generally, instantaneous fields for $g_o = 1$ are similar to those for $g_o = 1.4$, but only in the near-wake field. When $f_e/f_o = 1.0$, the instantaneous vorticity fields for $g_o = 1$ (Fig. 17) are similar to the previous cases with the same frequency ratio as shown in Figs. 9 and 13.

Fig. 18 shows the instantaneous vorticity fields for v and $f_e/f_o = 1.2$. While the wake patterns for $g_o = 1.8$ and $g_o = 1.4$ show periodicity with modulation of the drag and lift coefficients, those for $g_o = 1$ show unclear signs of modulation with rather regular drag and lift coefficients. After merging of the two rows of streets, the wake pattern became similar to that of a single bluff-body with one row of counter-rotating vortices. For $g_o = 1$, 'single bluff-body', 'flip-flop', and 'anti-phased synchronized' patterns are found for $0.8 \leqslant f_e/f_o \leqslant 1.2$.

4.1.4. $g_o = 0.6$

Although the flow may be 3-D for $g \leqslant 4$ in the case of stationary cylinders (Kang, 2003), as the cylinders are oscillated and as the gap varies from 0.2 to 1.0, the strong oscillation can be expected to strengthen the spanwise coherence (Blackburn and Henderson, 1999), and help maintain the 2-D flow. For two stationary cylinders, the flow patterns at $g_o = 0.6$ include 'single bluff-body' and 'flip-flop' wake patterns (Kang, 2003). For two oscillating cylinders, the drag

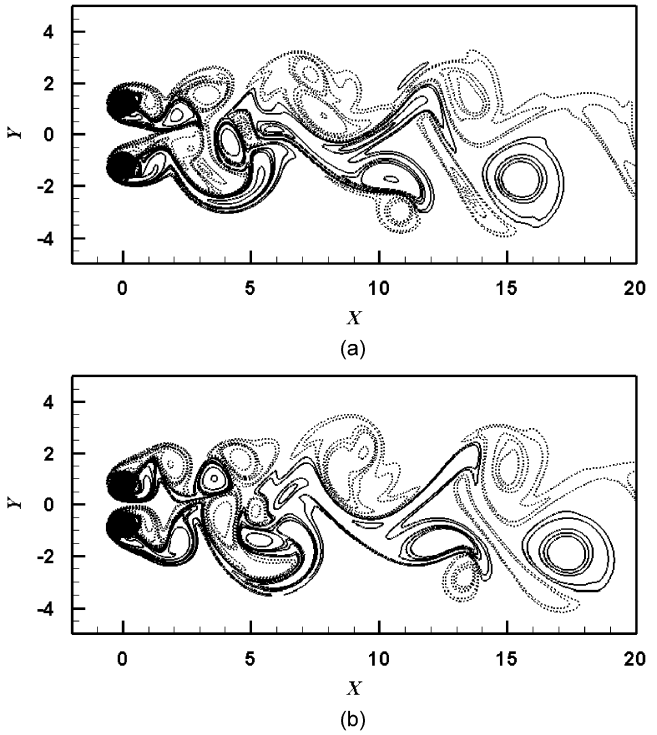

Fig. 18. Time series of instantaneous vorticity fields for $g_o = 1$ and $f_e/f_o = 1.2$ for (a) the furthest positions and (b) the closest positions.

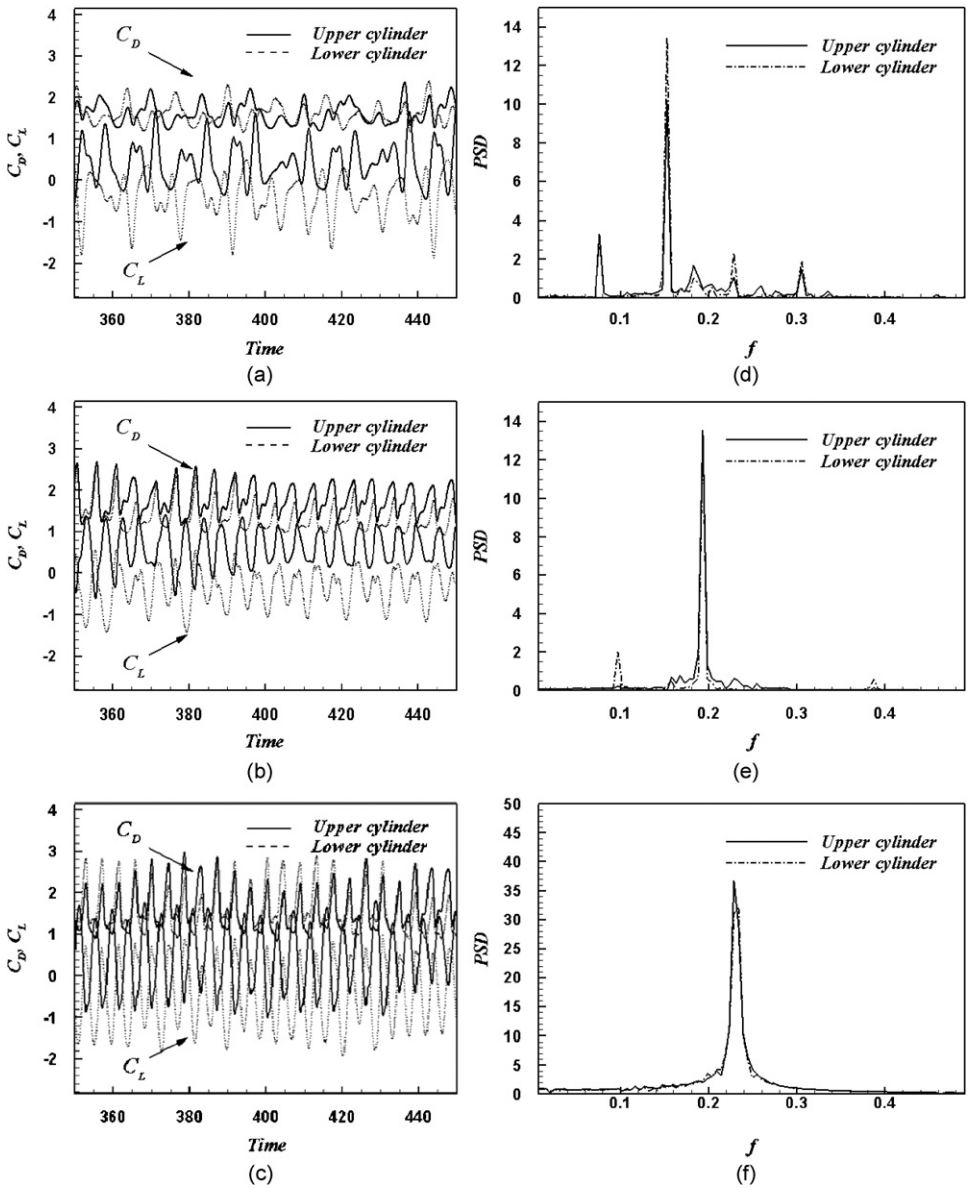

Fig. 19. Drag and lift coefficients (left column) and power spectra of lift coefficients (right column) for $g_o = 0.6$. In (a) and (d), $f_e/f_o = 0.8$; in (b) and (e), $f_e/f_o = 1.0$; in (c) and (f), $f_e/f_o = 1.2$.

and lift coefficients for $g_o = 0.6$ show 'single bluff-body' and 'deflected' patterns for $f_e/f_o = 0.8$ and $f_e/f_o = 1.0$ and 'single bluff-body' and 'flip-flop' patterns for $f_e/f_o = 1.2$. When $f_e/f_o = 0.8$, when the gap between the two cylinders is sufficiently small, vortex shedding is suppressed and shed vortices experience interference from each other. Thus, the drag and lift coefficients are random, as shown in Fig. 19(a). The Fourier transforms of the lift coefficients are presented in Fig. 19(d) and show primary peaks at $f = f_e$ with additional minor peaks at $\frac{1}{2}f_e, \frac{3}{2}f_e, 2f_e$. When f_e/f_o is 1.0, unlike other cases with same frequency ratio under wider gaps, the drag coefficients of the upper and lower cylinders are not the same and the lift coefficients are asymmetric about the centerline, as shown in Fig. 19(b). The Fourier transform of the lift coefficients has a primary peak at $f \approx f_e$ and a minor peak at $f \approx \frac{1}{2}f_e$, while other cases with the same frequency ratio and different gap spacings have a minor peak at $f \approx 2f_e$. Thus, we see signs of sub-harmonic instability in this case. When $f_e/f_o = 1.2$, the general pattern of the drag and lift coefficients for $g_o = 0.6$, as shown in Fig. 19(c), are similar to the case

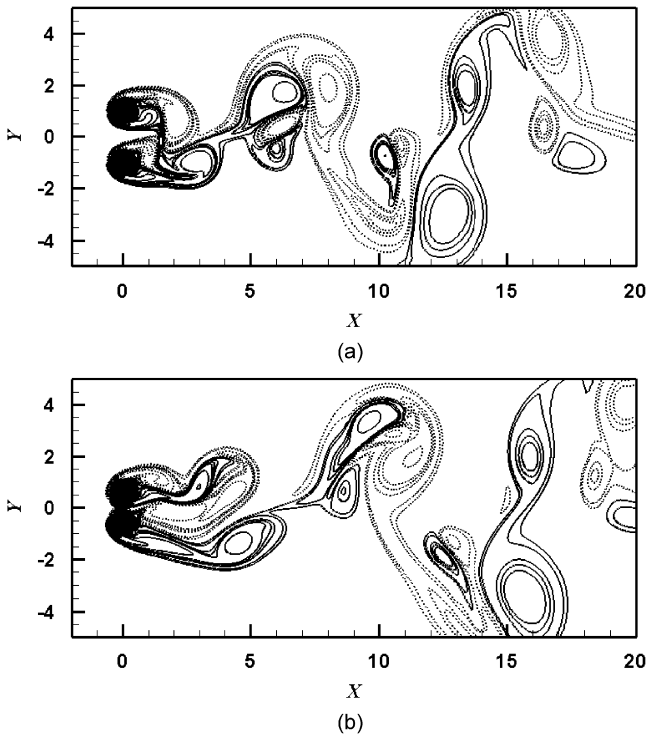

Fig. 20. Time series of instantaneous vorticity fields for $g_o = 0.6$ and $f_e/f_o = 0.8$ for (a) the furthest positions and (b) the closest positions.

of $g_o = 1$ and the modulation has nearly disappeared. The Fourier transforms of the lift coefficients are shown in Fig. 19(f) and show one primary peak at $f \approx f_e$. Thus, all the cases for $g_o = 0.6$ are of the lock-in type.

Figs. 20–22 show the instantaneous vorticity fields at $f_e/f_o = 0.8$, 1.0, and 1.2, respectively, for $g_o = 0.6$. The upper outer vortex is developing around the upper cylinder and the lower outer vortex is about to be shed at the instant shown in Fig. 20(a). From the time history of the drag coefficient shown in Fig. 19(a), we see flip-flopping behavior. Based on this, the lower outer vortex is expected to develop around the lower cylinder in a similar manner at a corresponding later time (not shown in this paper). For the case of $f_e/f_o = 1.0$, the inner vortices are deflected to the upper cylinder, as shown in Fig. 21(a and b), and the drag coefficient of the upper cylinder is greater than that of the lower cylinder, as shown in Fig. 19(b). Similarly, when $f_e/f_o = 1.2$, the inner vortices are deflected, as shown in Figs. 22(a and b) and 19(c). Suppression of the inner vortices is inhibited because of the small gap, as shown in Figs. 20(b), 21(b), and 22(b). For all frequency ratios for $g_o = 0.6$, we observe a 'single bluff-body' pattern of shedding.

The flow patterns and power spectra of the lift coefficients are summarized in Tables 1 and 2, respectively. Table 1 shows the wake patterns classified based on the two parameters, gap between the two cylinders and frequency ratio. The names of the shedding patterns are from Kang (2003) based on the results of two stationary cylinders-*S* is for 'anti- or in-phase synchronized', *F* for 'flip-flop', *D* for 'deflected', and *O* for 'single bluff-body'. Generally, for the same gap, oscillating and stationary cylinders have the same type of wake pattern. At $f_e/f_o = 1.0$, the flow patterns of the stationary cylinders for same gap appear, while unexpected patterns appear for lower or higher frequency ratios. According to Kang (2003), a deflected pattern appears for $f_e/f_o = 0.8$ and $g_o = 1.4$ at $\mathrm{Re} = 185$ and at $\mathrm{Re} = 70$ and $g = 0.5$ for two stationary cylinders. Therefore, more cases with various gaps, frequency ratios, and Reynolds numbers are needed to determine the effects of gap and frequency ratio.

Table 2 shows the summary of peak values of the power spectra of the lift coefficients. For $f_e/f_o = 0.8$, f_o is the primary peak except for $g_o = 0.6$, where the gap is too small for independent vortex shedding, and as a result the shedding is not in 'lock-in' status. The other cases with $f_e/f_o = 1.0$ and 1.2 have primary peaks at the oscillating frequency, so they are in the lock-in regime. Due to interferences of vortex shedding from each cylinder at smaller gaps, the natural frequency disappears for $f_e/f_o = 0.8$ and 1.2.

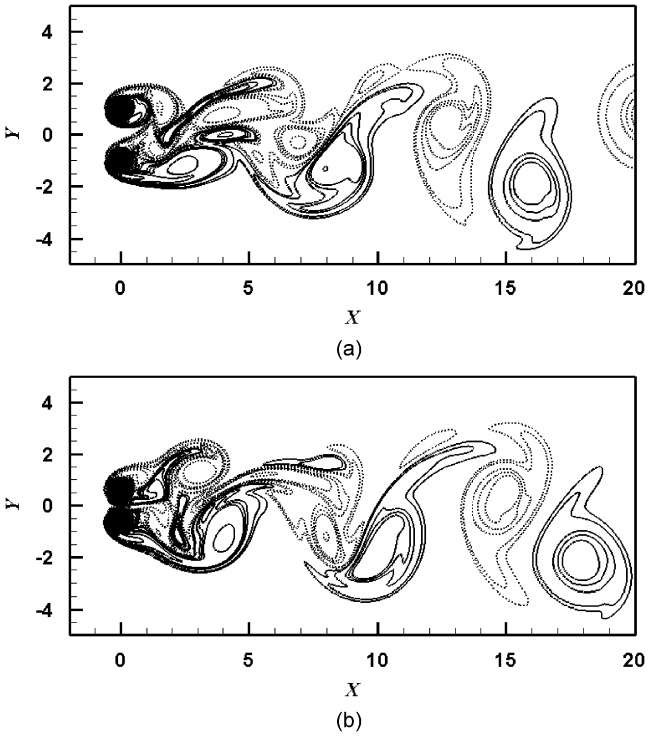

Fig. 21. Time series of instantaneous vorticity fields for $g_o = 0.6$ and $f_e/f_o = 1.0$ for (a) the furthest positions and (b) the closest positions.

4.2. Hydrodynamic forces

The upper and lower drag coefficients for the oscillating cylinders integrated over time are shown in Fig. 23(a) as a function of g for the stationary cylinders and g_o, the mean gap between the two cylinders. For $f_e/f_o = 0.8$, the drag coefficients decrease as g_o approaches 1.0, diverge to higher and lower values for lower and upper cylinder, respectively, up to 1.4, and then converge at $g_o = 1.8$. The drag coefficients are similar to those of stationary cylinders for $g_o > 1.8$. For $f_e/f_o \geqslant 1.0$ and $g_o \geqslant 0.6$, oscillating cylinders have higher drag coefficients than the corresponding stationary cases.

Fig. 23(b) shows the r.m.s. values of the drag coefficients for each cylinder. As the gap increases and as the cylinder is excited with lower frequencies, fluctuations in the drag coefficient decrease. All the oscillating cases have higher r.m.s. than the stationary cases. Fig. 23(c) shows the r.m.s. values of the lift coefficients. When f_e/f_o is >1.0, the oscillating cases have greater fluctuations in the lift coefficients than the other oscillatory or stationary cases. The single oscillating cylinder shows the same trend. The least value is obtained at $f_e/f_o = 1.0$ for two oscillating cylinders and at $f_e/f_o = 0.8$ for the single oscillating cylinder, as shown in Fig. 3.

5. Conclusions

Flow over two out-of-phase oscillating cylinders is numerically simulated using the immersed boundary method. The two cylinders oscillate out-of-phase at $\mathrm{Re} = 185$, and the ratio of amplitude to cylinder diameter is 0.2. The ratios of excitation frequency to natural vortex shedding frequency, f_e/f_o, and g to cylinder diameter, g, were systematically varied.

As expected, two oscillating cylinders have characteristics of two stationary cylinders and a single oscillating cylinder. Modulation phenomena appear for $f_e/f_o = 0.8$, while in a single oscillating cylinder, modulation is observed only for $f_e/f_o \geqslant 1.1$. For $f_e/f_o = 1.0$, except for the smallest gap case of $g_o = 0.6$, the characteristics are nearly the same for all the

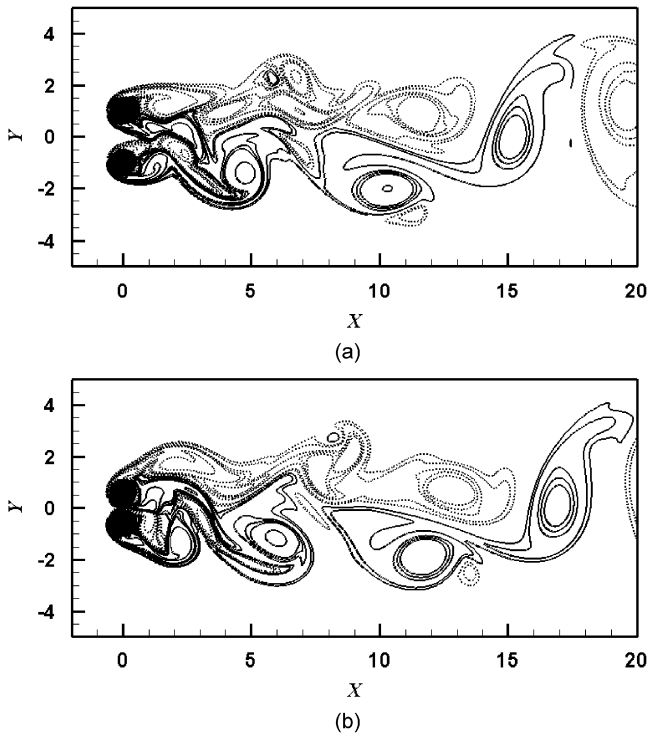

Fig. 22. Time series of instantaneous vorticity fields for $g_o = 0.6$ and $f_e/f_o = 1.2$ for (a) the furthest positions and (b) the closest positions.

Table 1
Wake patterns of two oscillating cylinders

	Stationary (Kang, 2003)	$f_e/f_o = 0.8$	$f_e/f_o = 1.0$	$f_e/f_o = 1.2$
$g_o = 1.8$	*S*	*S*	*S*	*F*, *S*
$g_o = 1.4$	*F*, *S*	*D*, *S*	*S*	*S*
$g_o = 1$	*F*, *S*	*F*	*S*	*O*, *F*, *S*
$g_o = 0.6$	*O*, *F*	*O*, *F*	*O*, *D*	*O*, *F*

Table 2
Peak values of Fourier transforms of lift coefficients of two oscillating cylinders

	$f_e/f_o = 0.8$	$f_e/f_o = 1.0$	$f_e/f_o = 1.2$
$g_o = 1.8$	f_o	f_e, $2f_e$	f_o, f_e
$g_o = 1.4$	f_o	f_e, $2f_e$	f_o, f_e
$g_o = 1$	f_o	f_e, $2f_e$	f_e
$g_o = 0.6$	$\frac{1}{2}f_e$, f_e, $\frac{3}{2}f_e$, $2f_e$	$\frac{1}{2}f_e$, f_e	f_e

gaps considered. For $f_e/f_o = 1.2$, modulation with beating is clear for the wide gap, similar to what was observed for a single oscillating cylinder.

Most of the wake patterns of two oscillating cylinders can be explained in terms of mechanisms observed for two stationary cylinders, a single oscillating cylinder, and their combinations. The near-wake can be classified with the previous classification for two stationary cylinders. However, 'in-phase synchronization', which can be found for two stationary cylinders over a similar parameter range, was not observed in the case of oscillating cylinders.

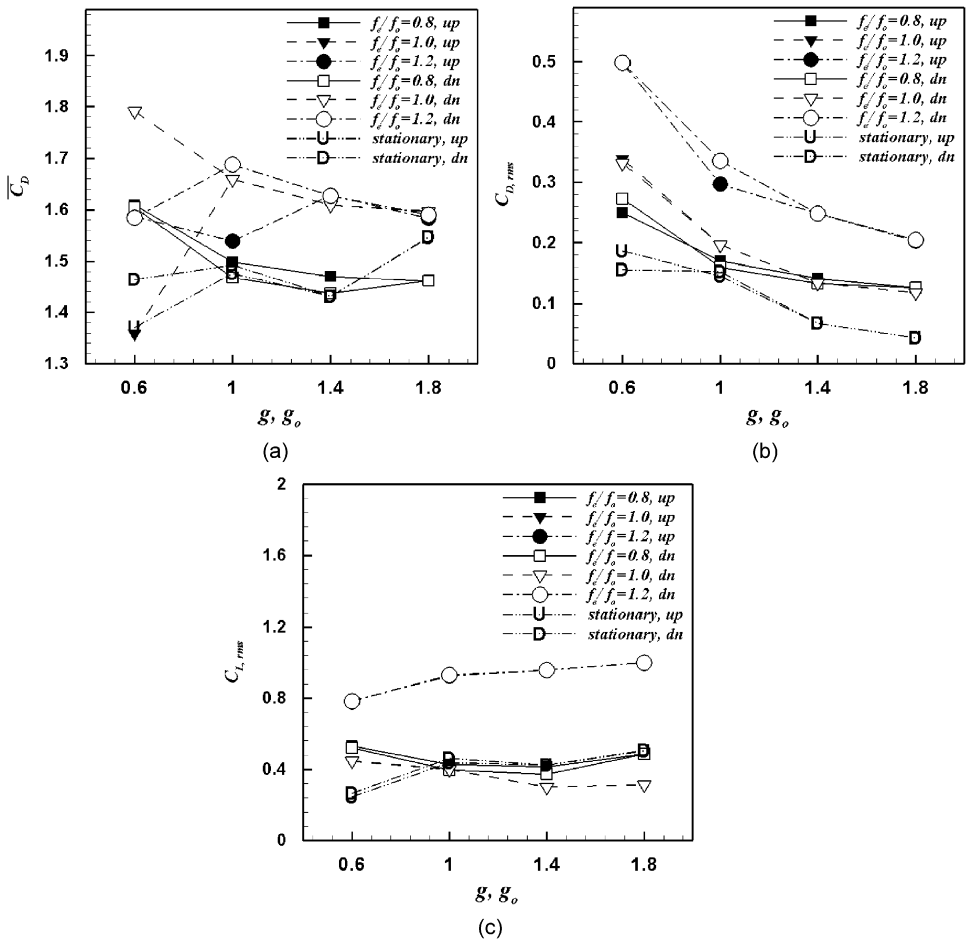

Fig. 23. (a) Time-averaged drag coefficients, (b) r.m.s. of drag coefficients, and (c) r.m.s. of lift coefficients as a function of frequency ratio and distance between two cylinders.

Most oscillating cylinders have higher drag and r.m.s. of drag and lift coefficients than stationary cylinders. The drag coefficients are affected by the oscillating frequency ratio and the gap distance, the r.m.s. of the drag coefficients is dominated by both the oscillating frequency ratio and gap, and the r.m.s. of the lift coefficients increase drastically when the frequency ratio is greater than 1.0.

Acknowledgements

This work was supported by the Korea Foundation for International Cooperation of Science & Technology (KICOS) through a grant provided by the Korean Ministry of Science & Technology (MOST) in 2007(2008) (No. K20702000013-07E0200-01310). Prof. Yoon thanks the Advanced Ship Engineering Research Center (ASERC) of Pusan National University for the financial support through the Korea Science and Engineering Foundation.

References

Anagnostopoulos, P., 2000. Numerical study of the flow past a cylinder excited transversely to the incident stream. Part 1: lock-in zoned, hydrodynamic forces and wake geometry. Journal of Fluids and Structures 14, 819–851.

Blackburn, H.M., Henderson, R.D., 1999. A study of two-dimensional flow past an oscillating cylinder. Journal of Fluid Mechanics 385, 255–286.

Gu, W., Chyu, C., Rockwell, D., 1994. Timing of vortex formation from an oscillating cylinder. Physics of Fluids 6 (11), 3677–3682.
Guilmineau, E., Queutey, P., 2002. A numerical simulation of vortex shedding from an oscillating circular cylinder. Journal of Fluids and Structures 16, 773–794.
Jester, W., Kallinderis, Y., 2004. Numerical study of incompressible flow about transversely oscillating cylinder pairs. ASME Journal of Offshore Mechanics and Arctic Engineering 126, 310–317.
Kang, S., 2003. Characteristics of flow over two circular cylinders in a side-by-side arrangement at low Reynolds numbers. Physics of Fluids 15, 2486–2498.
Khalak, A., Williamson, C.H.K., 1999. Motions, forces and mode transitions in vortex-induced vibrations at low mass-damping. Journal of Fluids and Structures 13, 813–851.
Kim, H.J., Durbin, P.A., 1988. Investigation of the flow between a pair of circular cylinders in the flopping regime. Journal of Fluid Mechanics 196, 431–448.
Kim, J., Moin, P., 1985. Application of a fractional-step method to incompressible Navier–Stokes Equation. Journal of Computational Physics 59, 308–323.
Kim, J., Kim, D., Choi, H., 2001. An immersed boundary finite-volume method for simulations of flow in complex geometries. Journal of Computational Physics 171, 132–150.
Leontini, J.S., Stewart, B.E., Thompson, M.C., Hourigan, K., 2006. Wake-state and energy transitions of an oscillating cylinder at low Reynolds number. Physics of fluids 18, 067101.
Mahir, N., Rockwell, D., 1996. Vortex formation from a forced system of two cylinders. Part II: side-by-side arrangement. Journal of Fluids and Structures 10, 491–500.
Meneghini, J.R., Bearman, P.W., 1995. Numerical simulation of high amplitude oscillatory flow about a circular cylinder. Journal of Fluids and Structures 9, 435–455.
Ponta, F.L., Aref, H., 2006. Numerical experiments on vortex shedding from an oscillating cylinder. Journal of Fluids and Structures 22, 327–344.
Sumner, D., Wong, S.S.T., Price, S.J., Paidoussis, M.P., 1999. Fluid behavior of side-by-side circular cylinders in steady cross-flow. Journal of Fluids and Structures 13, 309–338.
Toebes, G.H., 1969. The unsteady flow and wake near an oscillating cylinder. ASME Journal of Basic Engineering 91, 493–505.
Williamson, C.H.K., Roshko, A., 1988. Vortex formation in the wake of an oscillating cylinder. Journal of Fluids and Structures 2 (355), 355–381.
Zang, Y., Street, R.L., Koseff, J.R., 1994. A non-staggered grid, fractional step method for time-dependent incompressible Navier–Stokes equations in curvilinear coordinates. Journal of Computational Physics 114, 18–33.